Crystal structure of *cis*-prenyl chain elongating enzyme, undecaprenyl diphosphate synthase

Masahiro Fujihashi*, Yuan-Wei Zhang†, Yoshiki Higuchi*, Xiao-Yuan Li†, Tanetoshi Koyama†, and Kunio Miki*‡§

*Department of Chemistry, Graduate School of Science, Kyoto University, Sakyo-ku, Kyoto 606-8502, Japan; †Institute for Chemical Reaction Science, Tohoku University, Katahira 2-1-1, Aoba-ku, Sendai 980-8577, Japan; and ‡RIKEN Harima Institute/SPring-8, Koto 1-1-1, Mikazukicho, Sayo-gun, Hyogo 679-5148, Japan

Edited by Judith P. Klinman, University of California, Berkeley, CA, and approved January 25, 2001 (received for review October 27, 2000)

Undecaprenyl diphosphate synthase (UPS) catalyzes the *cis*-prenyl chain elongation onto *trans*, *trans*-farnesyl diphosphate (FPP) to produce undecaprenyl diphosphate (UPP), which is indispensable for the biosynthesis of bacterial cell walls. We report here the crystal structure of UPS as the only three-dimensional structure among *cis*-prenyl chain elongating enzymes. The structure is classified into a protein fold family and is completely different from the so-called "isoprenoid synthase fold" that is believed to be a common structure for the enzymes relating to isoprenoid biosynthesis. Conserved amino acid residues among *cis*-prenyl chain elongating enzymes are located around a large hydrophobic cleft in the UPS structure. A structural P-loop motif, which frequently appears in the various kinds of phosphate binding site, is found at the entrance of this cleft. The catalytic site is determined on the basis of these structural features, from which a possible reaction mechanism is proposed.

Over 23,000 structurally diverse isoprenoids are produced in nature, most of which are essential components of cellular machinery and serve as visual pigments, reproductive hormones, defensive agents, constituents of membranes, and signal transduction components. Prenyltransferases, so-called prenyl diphosphate synthases, catalyze the prenyl chain elongation of prenyl diphosphates that are the common precursors of the carbon skeletons for all isoprenoids. These enzymes can be classified into two major subgroups according to the *cis*- and *trans*-isomerism of products in the prenyl chain elongation (Fig. 1).

The structural genes for many kinds of prenyltransferases that catalyze *trans*-type prenyl chain elongation have been cloned and characterized (1). The amino acid sequence alignments of these enzymes have shown the presence of two characteristic aspartate-rich DDXXD motifs, which have been shown to be essential for the catalytic function as well as the substrate binding (2–6). The three-dimensional (3D) structure of farnesyl diphosphate synthase (FPS), a *trans*-type prenyltransferase, has been determined as the only structure in all prenyl chain elongating enzymes (7). Investigation of the FPS structure bound with the substrates also revealed that the aspartate-rich motifs are essential for catalysis (8).

On the other hand, little is known about the molecular mechanism and 3D structures of *cis*-type prenyl chain elongating enzymes. *cis*-Prenyl chain are indispensable for the biosynthesis of peptidoglycan in prokaryotes and that of glycoprotein in eukaryotes (Fig. 1; ref. 9). Deficiency of this biosynthesis results in the inhibition of cell wall biosynthesis in *Escherichia coli* and an abnormal accumulation of ER and Golgi membranes in yeast *Saccharomyces cerevisiae* (10, 11). Molecular cloning of the gene for undecaprenyl diphosphate synthase (UPS), which catalyzes the *cis*-prenyl chain elongation onto farnesyl diphosphate (FPP, C_{15}) to produce undecaprenyl diphosphate (UPP, C_{55}), has recently been carried out on an enzyme from *Micrococcus luteus* B-P 26 (12). The UPS gene from *E. coli* as well as from other bacteria was also identified shortly afterward (10, 13), and the *S. cerevisiae RER2* gene has been identified to encode a *cis*-prenyltransferase that is essential for the biosynthesis of dolichols (11). Comparison of the deduced primary structures of the *cis*-prenyltransferases reveals the presence of several conserved regions, which lack the DDXXD motif and are completely dissimilar to those of the *trans*-prenyltransferases (2–6, 13, 14).

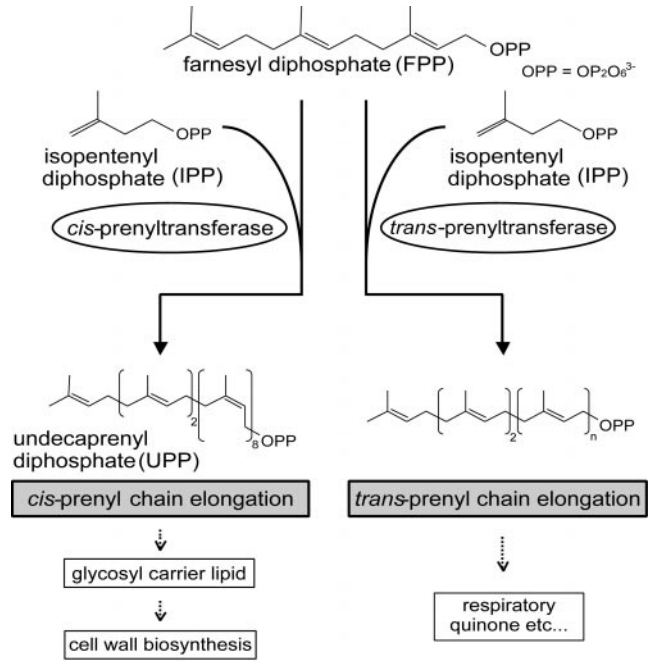

Fig. 1. A schematic drawing of the biosynthesis related to prenyl chains. UPS catalyzes 8× *cis*-prenyl chain elongation step by step. Both *cis*- and *trans*-prenyl chains are constructed from the same substrates by the *cis* or *trans* types of prenyltransferase, in which the only difference is the *cis*- and *trans*-isomerism of the prenyl chain product.

We report here the crystal structure of UPS from *M. luteus* B-P 26 as the only 3D structure in all *cis*-prenyl chain elongating enzymes, and discuss the molecular mechanism of *cis*-prenyltransferases.

Materials and Methods

Purification, Crystallization, and Data Collection. UPS from *M. luteus* B-P 26 was overproduced, purified, and crystallized as described (12, 15). Heavy atom derivatives were prepared by the soaking

This paper was submitted directly (Track II) to the PNAS office.

Abbreviations: UPS, undecaprenyl diphosphate synthase; FPS, farnesyl diphosphate synthase; FPP, farnesyl diphosphate; IPP, isopentenyl diphosphate; 3D, three-dimensional.

Data deposition: The atomic coordinates have been deposited in the Protein Data Bank, www.rcsb.org (PDB ID code 1F75).

§To whom reprint requests should be addressed. E-mail: miki@kuchem.kyoto-u.ac.jp.

The publication costs of this article were defrayed in part by page charge payment. This article must therefore be hereby marked "*advertisement*" in accordance with 18 U.S.C. §1734 solely to indicate this fact.

Table 1. X-ray data collection and phasing statistics

	Native	Thimerosal*	$KAu(CN)_2$
Data Collection			
Source	PF-BL6B	PF-BL6A	PF-BL6A
Wavelength, Å	1.000	1.000	1.000
Space group	*C*2	*C*2	*C*2
Cell constants			
a, b, c (Å)	127.1, 60.1, 75.7	127.3, 60.0, 75.5	127.1, 60.1, 75.6
β (°)	105.7	105.8	105.7
Resolution, Å†	100–2.2 (2.24–2.20)	100–3.1 (3.21–3.10)	100–3.2 (3.31–3.20)
Reflections, total/unique	57323/23530	24695/8239	24780/7530
Completeness, %	83.7 (56.8)	80.1 (56.2)	82.2 (58.5)
$\langle I/\sigma(I)\rangle$	24.3	8.4	9.9
R_{merge}, %‡	3.2 (16.8)	9.9 (31.5)	10.4 (33.5)
Phasing Statistics			
R_{iso}, %§		24.6	11.9
No. of sites		4	2
Phasing power¶ acentric/centric		1.76/1.59	0.82/0.74
Cullis*R*‖ acentric/centric		0.69/0.58	0.87/0.82
Cullis$R_{anomalous}$**		0.91	0.98
Mean figure of merit (20.0–3.1 Å)	0.43		

*$C_9H_9HgNaO_2S$.

†Values in parentheses are for the outmost resolution shell.

‡$R_{merge} = \Sigma|I_i - \langle I_i\rangle|/\Sigma\langle I_i\rangle$, where I_i is the observed intensity and $\langle I_i\rangle$ is the average intensity over symmetry equivalent measurements.

§$R_{iso} = \Sigma||F_{PH}| - |F_P||/\Sigma|F_P|$, where F_{PH} and F_P are the derivative and native structure factors, respectively.

¶Phasing power $= \langle|F_H|/||F_{PH}| - |F_P + F_H||\rangle$, where F_H, F_{PH} and F_P are the heavy atom, derivative and native structural factors, respectively.

‖Cullis $R = \langle||F_{PH}| - |F_P + F_H||\rangle/\langle||F_{PH}| - |F_P||\rangle$.

**Cullis$R_{anomalous} = \langle|F_{PH}(+) - F_{PH}(-)| - 2 \times F_H \times \sin\alpha_P\rangle/\langle|F_{PH}(+) - F_{PH}(-)|\rangle$, where α_P is the protein phase.

method. For both thimerosal and $KAu(CN)_2$ derivatives, the concentration of heavy atom compounds in the soaking buffer and the soaking periods were 1 mM and 1 day, respectively. Diffraction studies were performed at room temperature at the Photon Factory (BL6A and BL6B) and SPring-8 (BL40B2). Data were reduced by using DENZO, SCALEPACK (16), and TRUNCATE (17) (Table 1).

Structure Analysis. Phasing was accomplished by multiple isomorphous replacement with anomalous scattering using MLPHARE (17). The structural model was constructed by using O (18), and refined by X-PLOR with bulk solvent corrections (ref. 19; Table 2). Accessible surface area was calculated by using SURFACE (17). A 3D structural homology search was performed by using the DALI algorithm (20). The monomer and the dimer of polyglycine model coordinates were submitted to the DALI server (http://www2.ebi.ac.uk/dali/dali.html). The superimposition of the dimer was performed by using the program LSQMAN (21).

Table 2. Refinement statistics

Refinement statistics	
Resolution, Å	50.0–2.2
R, %/R_{free}, %*	19.0/24.6
No. of atoms	
protein	3508
ligand	10
solvent	38
Model statistics	
rms bond length, Å	0.006
rms bond angles, °	1.120
Ramachandran angles most favored, %	92.1
Ramachandran angles additional allowed, %	7.3

R_{free} is the same as R, but for a 5% subset of all reflections that were never used in crystallographic refinement.

*$R = \Sigma||F_{obs}| - |F_{calc}||/\Sigma|F_{obs}|$.

Overall Structure of UPS

The overall structure of UPS from *M. luteus* B-P 26 was determined at 2.2 Å resolution by multiple isomorphous replacement with anomalous scattering (MIRAS) (Table 2 and Fig. 2 *A* and *B*). This enzyme acts as a homodimer of 29-kDa subunits under physiological conditions (12, 22). The asymmetric unit contains one homodimer, in which each monomer is crystallographically independent. The front view of the dimeric form of UPS looks like the face of an elephant (Fig. 2*A*). The contact interface of the dimer is about 15%. The topology diagram of the secondary structures shows that the monomer has six parallel β-strands (S1–S6) and seven α-helices (H1, H2, H3, H5, H6, H8, and H10) (Fig. 2*C*). The β-strands form a central β-sheet core, which is surrounded by five of the seven α-helices (H1, H2, H3, H5, and H10). Additionally, there are three short 3_{10}-helices (H4, H7, and H9) in each monomer. The N-terminal residues 1M to 13N of one monomer and 1M to 18A of the other monomer, residues from 74S to 85V of both monomers, and the C-terminal 243H to 249L of both monomers could not be incorporated in the structural model because of poor electron densities.

The fold of UPS is completely different from those of other isoprenoid biosynthesis-related enzymes. These enzymes, which include FPS (7, 8), pentalenene synthases (23), 5-epi-aristolochene synthases (24), squalene cyclase (25), and protein farnesyltransferase (26), have a common structural motif. This motif is called the isoprenoid synthase fold (or terpenoids synthase fold) (27, 28), and has been believed to be included in all enzymes related to isoprenoid biosynthesis. It is composed of ten to twelve mostly antiparallel α-helices. However, UPS of the present study has a central β-sheet core, which is a different from the isoprenoid synthase fold. Additionally, it

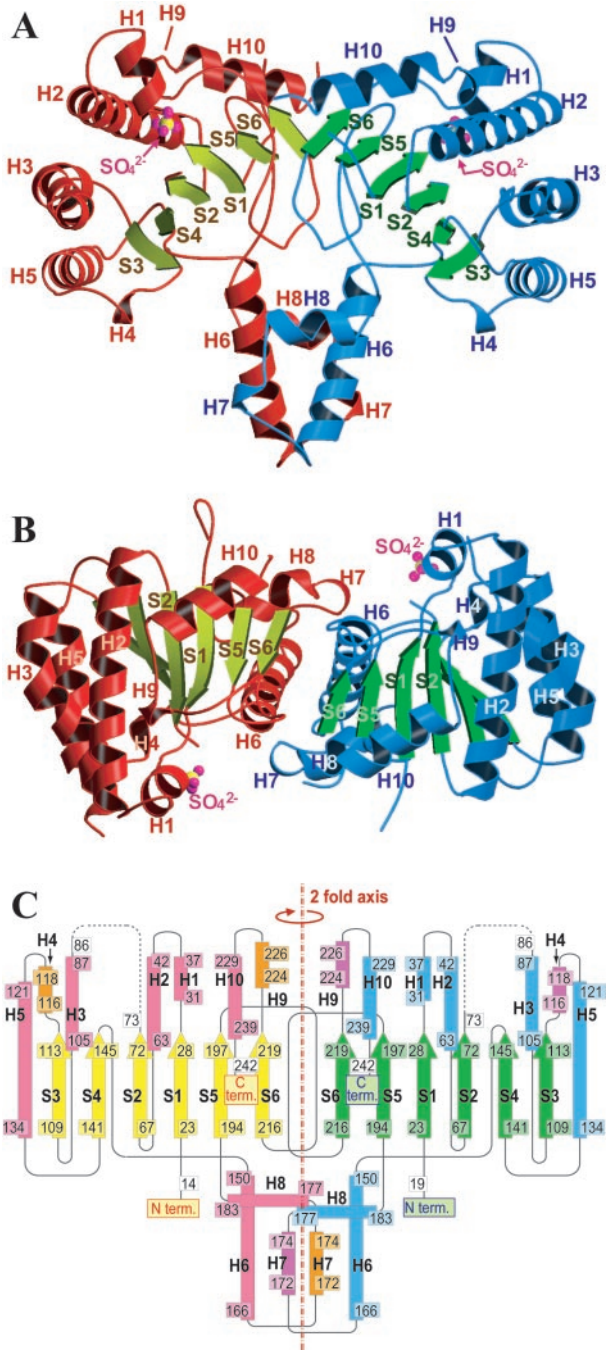

Fig. 2. Overall structure of UPS from *M. luteus* B-P 26. A front view (*A*) and a top view (*B*) of the dimer structure (ribbon model). One monomer of UPS is shown by red helices (α- and 3_{10}-helices) and yellowish green arrows (β-strands), and the other monomer by blue helices and green arrows. Helices (H1–H10) and strands (S1–S6) are labeled together with the sulfate ions found in the crystal structure. These two figures were prepared with MOLSCRIPT (33) and RASTER3D (34). (*C*) A topology diagram of the secondary structure of the UPS dimer. α- and 3_{10}-helices of one monomer and those of the other monomer are colored pink, orange, sky-blue, and light purple, respectively. β-strands of one monomer and the other are colored yellow and green, respectively.

was found that UPS belongs to a new protein folding family, judging from the multiple alignment of 3D structural neighbors search. This suggests that the catalytic mechanisms of UPS, including substrate recognition, are also different from those of other enzymes related to isoprenoid biosynthesis.

Substrate Binding Site

Both FPP and isopentenyl diphosphate (IPP), the substrates of UPS, consist of negatively charged diphosphates and hydrophobic carbon chains. Thus, it is clear that the diphosphates must be recognized by positively charged residues, and the carbon chains must be bound to hydrophobic residues. As shown in Fig. 3*A*, UPS has a large cleft on its molecular surface that is surrounded by the S2 and S4 strands and the H2 and H3 helices. Most of the conserved amino acid residues among *cis*-prenyltransferases are located in this cleft (Fig. 3*A*). The interior of the cleft mainly consists of hydrophobic residues. Four arginine residues (R33, R42, R197, and R203) located at the entrance of the cleft form a positively charged cluster. This cleft seems to be suitable for recognition of the substrates, as hereafter discussed.

At the entrance of this cleft was found a common motif for phosphate recognition called a structural P-loop. Structural P-loop motifs are found in many phosphate-binding enzymes, such as nucleotide triphosphate hydrolase, phosphofructokinase, c-AMP binding domain, and sugar phosphatase (29). This motif generally consists of four residues located in the N terminus of an α-helix, in which glycine at the N terminus is followed by three strongly conserved residues among related enzymes with similar functions. In the UPS structure, the P-loop motif is composed of 30G, 31N, 32G, and 33R located at the N terminus of the H1 helix. Three of four P-loop residues (30G, 31N, and 33R) are strictly conserved among *cis*-prenyltransferases as shown in Fig. 3*B*. On the other hand, Gly and Arg are alternatively located at the positions corresponding to the 32nd residue (in the *M. luteus* UPS sequence) (Fig. 3*B*), which is located close to the 42nd residue in the 3D structure (Fig. 3*C*). Interestingly, in many *cis*-prenyltransferases that have Gly at the position corresponding to the 32nd, Arg is always located at the position corresponding to the 42nd, whereas the residue is not specified when the residue corresponding to the 32nd is Arg (Fig. 3*B*). In UPS from *M. luteus*, 42R is one of the arginine residues in the positively charged cluster at the entrance of the cleft, and it is close to 32G as shown in Fig. 3*C*. When 32G is replaced with arginine in *cis*-prenyltransferases, the guanidinium group of the replaced arginine (32R) may occupy the space for the guanidinium group of 42R (Fig. 3*D*). This indicates that Arg at the 32nd or 42nd position in the 3D structure is complementarily conserved among *cis*-prenyltransferases. In other words, at the entrance of the cleft, an arginine residue is conserved in the restricted position to recognize the diphosphate group of the substrates for this enzyme.

Moreover, a sulfate ion used in crystallization as a precipitant (15) binds to the four residues of the P-loop motif (Fig. 3*C*). The electron density for this ion is larger than that of water and it is not located near the main chain O atoms but is surrounded by the main chain N atoms of the P-loop residues and also by the guanidinium group of R33. These main chain N atoms of 30G, 31N, 32G, and 33R and the guanidinium group of 33R could be hydrogen bonded to the O atoms of the sulfate ion. It has been reported that the main chain N atoms of the four residues of the P-loop motif usually bind to the phosphate group of the substrates of many phosphate-binding enzymes (29). These observations suggest that the diphosphate group of the substrate is electrostatically recognized by the P-loop motif in the same position where the sulfate ion is located.

The catalytic site might be highly flexible, which is necessary for substrate recognitions, catalytic reactions, and product releases. The residues from 74S to 85V could not be incorporated even in the finally refined model because of their invisible electron densities. As deduced from the positions of 73F and 86N, these undefined residues are assumed to be located near the cleft (Fig. 3*A*). The superposition of the two equivalent mono-

BIOCHEMISTRY

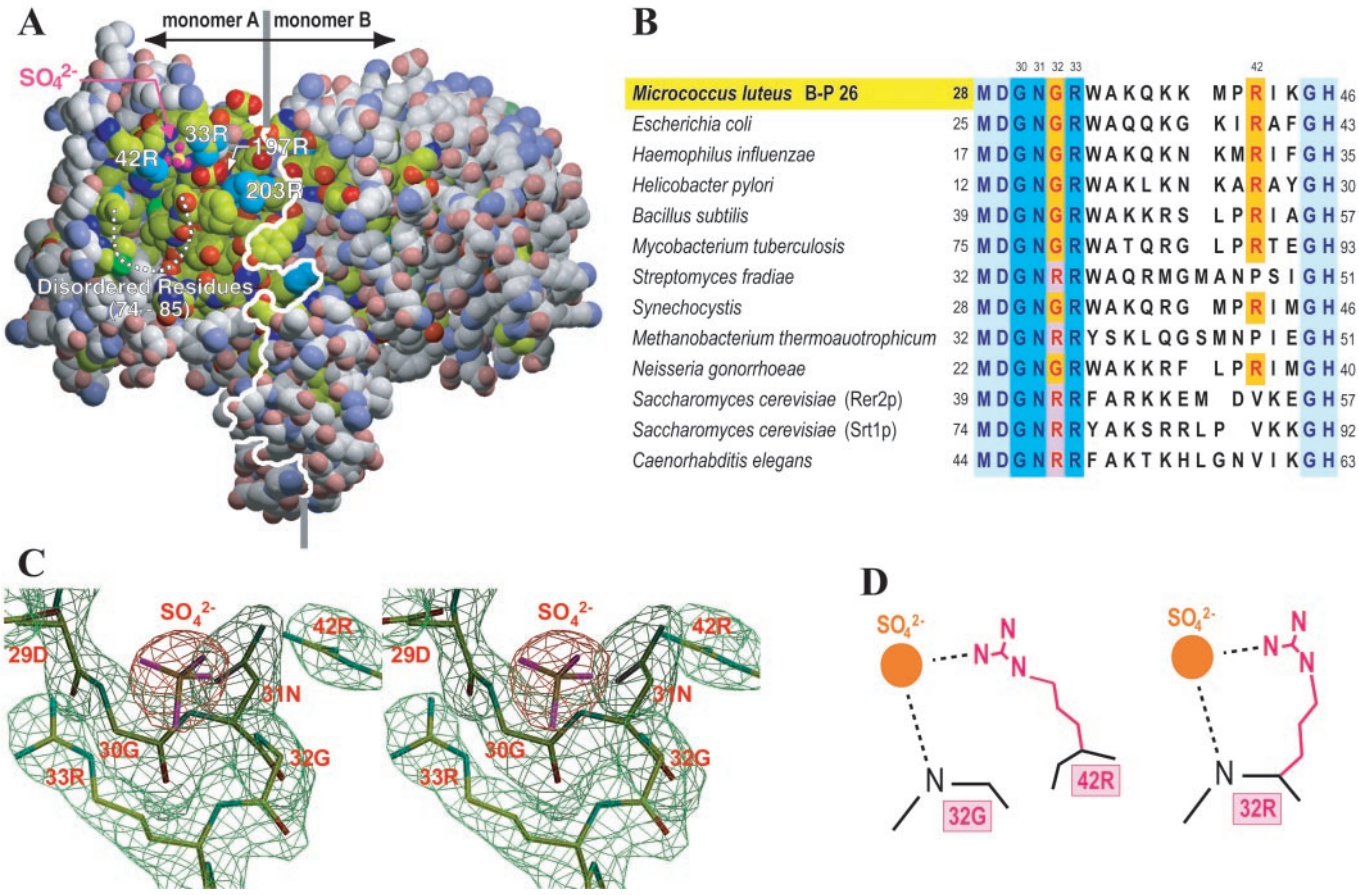

Fig. 3. Active site in the UPS structure. (*A*) Space filling model of the UPS dimer. C atoms are indicated in yellowish green and gray, in which the former color corresponds to conserved residues and the latter nonconserved residues among the *cis*-prenyltransferase family. These conserved residues form a large hydrophobic cleft. N, O, and S atoms are colored in blue, red, and green, respectively. The white line indicates the interface of the dimer, where the left and right monomers are named A and B. White dotted line shows the disordered residues from 74S to 85V. This figure was prepared in the same manner as Fig. 2 *A* and *B*. (*B*) A comparison of amino acid sequences in 13 proteins that have sequence homology with UPS from *M. luteus* B-P 26 (12, 13). Only residues corresponding to 28–46 of *M. luteus* UPS are presented. The proteins from *M. luteus*, *E. coli*, and *Hemophilus influenzae* demonstrate UPS activity (10, 12, 13). RER2p from *S. cerevisiae* has *cis*-prenyltransferase activity (11). The others are potential *cis*-prenyltransferases homologous with *M. luteus* UPS. (*C*) Stereo view of the electron density map around the structural P-loop motif and the sulfate ion. The final refined structure is superimposed. (*D*) Three-dimensionally conserved guanidinium head of arginine. The positively charged guanidinium group of either 42R (in the case of 32G; *Left*) or 32R (in the case of 32R; *Right*) binds to the diphosphate head of the substrate.

mers in the dimer shows that most of the Cα atoms are well superimposed on each other (rmsd of Cα atoms = 0.49 Å) except for the region from 86N to 95F, which is adjacent to the disordered loop. It is noteworthy that the residues between 71Y and 91L, which are highly conserved among *cis*-prenyltransferases (13), show a high mobility (average *B* factor = 66.8 Å^2) in the UPS structure. Additionally, one of the cluster arginines, 42R, which is a residue complementarily conserved with 32G and in close contact with the sulfate ion, also has a large B factor (B = 74.8 Å^2). Each 42R in the two monomers shows different features in binding with the sulfate ion. The guanidinium group of 42R in one monomer is hydrogen-bonded to the O atoms of the sulfate ion. On the other hand, no atoms of 42R in the other monomer interact directly with the sulfate ion. However, the electron density of the side chain of 42R is very broad, suggesting the existence of several side chain conformers. The guanidinium group of 42R in one such conformer can bind to the sulfate. The high flexibility around this cleft must play an essential role in catalytic reactions.

Site-directed mutagenesis analysis also supports that this cleft is the catalytic site of UPS (30). Substitutions of 77N significantly decrease the k_{cat} value and that of 78W increase the K_m value for FPP. These results indicate that 77N plays an important role in catalytic reaction, and that 78W is the binding residue with FPP (30). Although these two residues could not be incorporated into the final refined structure, positions of 73F and 86N suggest that 77N and 78W must locate at the front of this cleft (Fig. 3*A*).

Catalytic Mechanism

A plausible substrate-binding model is shown in Fig. 4. In this model, the hydrophobic carbon chain of FPP is recognized by the hydrophobic cleft, which has a suitable volume to accommodate elongating states of the allylic substrate. Deduced from locations of this cleft and the structural P-loop motif, the main chain N atoms of 30G, 31N, 32G, and 33R bind to the diphosphate group of FPP. The guanidinium group of 33R also interacts to this diphosphate group. It is shown that UPS requires the magnesium ion for the catalytic activity (31). In this model, a magnesium bridge could be formed between the carboxyl group of 29D and the diphosphate part of the allylic substrate as found in the case of FPS (8). On the other hand, the diphosphate group of the

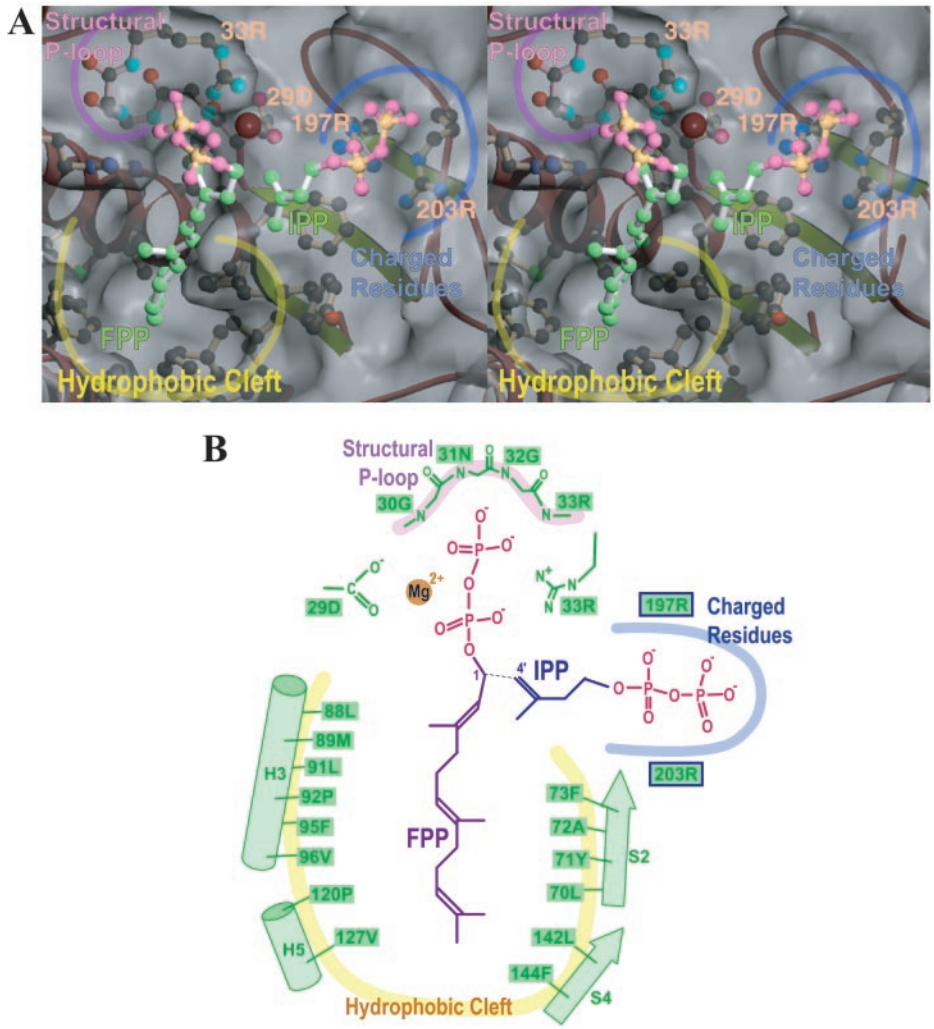

Fig. 4. Hypothetical FPP and IPP binding model with UPS. (*A*) Stereo view of the molecular surface of UPS (gray envelope) and the bindings of FPP and IPP (C, O, and P atoms in green, pink, and orange, respectively). The estimated position of the magnesium ion is shown by the brown sphere. This figure was prepared by using MOLSCRIPT (33), GRASP (35), and RASTER3D (34). (*B*) Schematic presentation of a binding model. The UPS structure is shown in green.

substrate IPP could interact with the positively charged residues, 197R and 203R. Except for these arginines, no conserved residues that could bind with the diphosphate part of IPP are found around the FPP binding position.

The condensation reaction may be triggered by the release of the diphosphate group of FPP as previously observed in the FPS reaction (32). This release produces the allylic farnesyl cation, and then the covalent bond could be formed between the C1 atom of FPP and the C4′ atom of IPP. By repetition of this stereochemically controlled reaction, the *cis*-prenyl chain must be elongated until the hydrophobic carbon chain reaches the fixed length of C_{55} by moving into the inside of the hydrophobic cleft. The final product undecaprenyl diphosphate (UPP) may be bound to the cleft in a bent conformation, and the final chain length is determined by the size of this hydrophobic cleft.

We thank K. Fujikura and Y. Kharel for their biochemical experiments, and Drs. N. Sakabe, N. Watanabe, M. Suzuki, N. Igarashi, and K. Miura for their help in diffraction studies at Photon Factory and SPring-8 (Proposal Nos. 2000G131 and 2000A0294, respectively). K.M. is a member of the Structural Biology Sakabe Project, University of Tsukuba. This work was supported by the Research for the Future Program (97L00501 to K.M. and 97I00302 to T.K.) from the Japan Society for the Promotion of Science, the Ground Research for Space Utilization Program (to K.M.) from National Space Development Agency of Japan and the Japan Space Forum, and Grant-in-Aid for Encouragement of Young Scientist (to Y.-W. Z.) from the Ministry of Education, Science, Sports and Culture of Japan.

1. Ogura, K. & Koyama, T. (1998) *Chem. Rev.* **98,** 1263–1276.
2. Carattoli, A., Romano, N., Ballario, P., Morelli, G. & Macino, G. (1991) *J. Biol. Chem.* **266,** 5854–5859.
3. Joly, A. & Edwards, P. A. (1993) *J. Biol. Chem.* **268,** 26983–26989.
4. Koyama, T., Obata, S., Osabe, M., Takeshita, A., Yokoyama, K., Uchida, M., Nishino, T. & Ogura, K. (1993) *J. Biochem. (Tokyo)* **113,** 355–363.
5. Song, L. & Poulter, C. D. (1994) *Proc. Natl. Acad. Sci. USA* **91,** 3044–3048.
6. Koyama, T., Tajima, M., Sano, H., Doi, T., Koike-Takeshita, A., Obata, S., Nishino, T. & Ogura, K. (1996) *Biochemistry* **35,** 9533–9538.
7. Tarshis, L. C., Yan, M., Poulter, C. D. & Sacchettini, J. C. (1994) *Biochemistry* **33,** 10871–10877.
8. Tarshis, L. C., Proteau, P. J., Kellogg, B. A., Sacchettini, J. C. & Poulter, C. D. (1996) *Proc. Natl. Acad. Sci. USA* **93,** 15018–15023.
9. Bugg, T. D. & Brandish, P. E. (1994) *FEMS Microbiol. Lett.* **119,** 255–262.
10. Kato, J., Fujisaki, S., Nakajima, K., Nishimura, Y., Sato, M. & Nakano, A. (1999) *J. Bacteriol.* **181,** 2733–2738.
11. Sato, M., Sato, K., Nishikawa, S., Hirata, A., Kato, J. & Nakano, A. (1999) *Mol. Cell. Biol.* **19,** 471–483.

12. Shimizu, N., Koyama, T. & Ogura, K. (1998) *J. Biol. Chem.* **273,** 19476–19481.
13. Apfel, C. M., Takacs, B., Fountoulakis, M., Stieger, M. & Keck, W. (1999) *J. Bacteriol.* **181,** 483–492.
14. Chen, A., Kroon, P. A. & Poulter, C. D. (1994) *Protein Sci.* **3,** 600–607.
15. Fujihashi, M., Shimizu, N., Zhang, Y.-W., Koyama, T. & Miki, K. (1999) *Acta Crystallogr. D* **55,** 1606–1607.
16. Otwinowski, Z. & Minor, W. (1997) *Methods Enzymol.* **276,** 307–326.
17. Collaborative Computational Project, Number 4 (1994) *Acta Crystallogr. D* **50,** 760–763.
18. Jones, T. A., Zou, J. Y., Cowan, S. W. & Kjeldgaard, M. (1991) *Acta Crystallogr. A* **47,** 110–119.
19. Brünger, A. T. (1992) *X-PLOR, A System for X-Ray Crystallography and NMR* (Yale Univ. Press, New Haven, CT).
20. Holm, L. & Sander, C. (1995) *Trends Biochem. Sci.* **20,** 478–480.
21. Kleywegt, G. J. (1996) *Acta Crystallogr. D* **52,** 842–857.
22. Muth, J. D. & Allen, C. M. (1984) *Arch. Biochem. Biophys.* **230,** 49–60.
23. Lesburg, C. A., Zhai, G., Cane, D. E. & Christianson, D. W. (1997) *Science* **277,** 1820–1824.
24. Starks, C. M., Back, K., Chappell, J. & Noel, J. P. (1997) *Science* **277,** 1815–1820.
25. Wendt, K. U., Poralla, K. & Schulz, G. E. (1997) *Science* **277,** 1811–1815.
26. Park, H. W., Boduluri, S. R., Moomaw, J. F., Casey, P. J. & Beese, L. S. (1997) *Science* **275,** 1800–1804.
27. Sacchettini, J. C. & Poulter, C. D. (1997) *Science* **277,** 1788–1789.
28. Wang, K. & Ohnuma, S. (1999) *Trends Biochem. Sci.* **24,** 445–451.
29. Kinoshita, K., Sadanami, K., Kidera, A. & Go, N. (1999) *Protein Eng.* **12,** 11–14.
30. Fujikura, K., Zhang, Y.-W., Yoshizaki, H., Nishino, T. & Koyama, T. (2000) *J. Biochem. (Tokyo)* **128,** 917–922.
31. Allen, C. M., Keenan, M. V. & Sack, J. (1976) *Arch. Biochem. Biophys.* **175,** 236–248.
32. Poulter, C. D. & Rilling, H. C. (1978) *Acc. Chem. Res.* **11,** 307–313.
33. Kraulis, P. J. (1991) *J. Appl. Crystallogr.* **24,** 946–950.
34. Merritt, E. A. & Bacon, D. J. (1997) *Methods Enzymol.* **277,** 505–524.
35. Nicholls, A., Sharp, K. A. & Honig, B. (1991) *Proteins* **11,** 281–296.